Development of a Microfluidic Device to Improve Microfiltration Process

Achmad Rohyani[1], Philippe Schmitz[1], and Christine Lafforgue[1]

Abstract—*When neutrally buoyant particles are subjected in laminar and continuous flow, one can observe that particles generally migrate across the streamlines in a particular way. Such lateral motion called "tubular-pinched effect" causes particles tend to migrate toward micro channel wall. The origin of this motion is due to the parabolic nature of the laminar velocity profile in Poiseuille flow. This phenomenon produces a shear-induced inertial lift forces which allows the scattered particles focused and form narrow annulus near the wall. The focalization of particles could improve the method of separation process by using microfiltration. Then, micro porous membrane is used for microfiltration which filters focused particles from a fluid by passage through it. In this work, we use this lift forces generated in laminar microfluidic systems to focus randomly distributed particles continuously. The form of particles deposition poon micro porous membrane hence was observed to determine the important parameter influencing the equilibrium position of the particles. A numerical simulation (COMSOL Multiphysics ®) has also first been developed to study the influence of channel and on the subsequent size of annulus formed by the focused particles on the membrane.*

Keywords—hydrodynamic lift, equilibrium position, particle separation.

I. INTRODUCTION

Fundamental advances in the development of the microfluidic process in cell and particle handling have proven to be very useful. The knowledge in this field have been demonstrated to be important for a wide range of applications such as manipulation and separation of micro particles, both biological and synthetic, in the domain of industry, biology and medicine[1]. Recently, microfluidic systems have a great interest for particle handling with increased control and sensitivity. The main advantages of miniaturized systems include smallness of volume, ease-of-use, point-of-care diagnostics, fast reaction of a sample, and so forth, which can be found elsewhere. Many practical microfluidic applications are necessarily associated with two-phase flows. In practice, this device often transport particulate samples, i.e. blood cells, bacteria, DNAs, and spherical particles of sizes up to 10 μm in a micro channel with a characteristic length scale of hundred microns for small but finite Reynolds number operations[2]. This circumstance leads to solid-liquid two-phase flows because the small length scale effect produces a high shear rate in micro channels.

The particles subjected in the fluid will be experienced forces exerted by the flow of the fluid. Under laminar flow conditions, neutrally buoyant particle will not necessarily follow fluid streamlines due to the parabolic profile of the streamlines. Consequently, the particle move laterally toward the micro channel wall because of the shear stress gradient. At the near wall, due to rotational wakes around the particles disturbed, the particles will stay at their equilibrium position near the wall along the streamlines. The effect was called "tubular pinch effect", because of the tube like shape of the annular region to which particles migrate. It was observed that the narrow annulus at a position 0.6 times the radius of the pipes[3].

Many researches have been conducted to study this phenomenon. In general, it is suggested that the equilibrium position and particle distribution are influenced by parameters such as the channel-to-particle size ratio, particle density, particle volume fraction, Re, etc. The channel-to-particle size ratio influence the equilibrium position since it correlate with the shear rate of the fluid relative to the force experienced by the particles. This force depends on particle size, channel dimensions and flow velocity. As for the influence of particle density, which has been considered only with regard to vertical channel systems, a lighter particle will leads the upward flowing fluid reaches near the channel wall but a heavier one lags behind and migrates toward the channel axis. Effect of the particle volume fraction, the existence of the particle suspension will disrupt flow path due to particle interaction. A particle will not be able to move freely as limited by its surrounding neighbors. However, the effect of particle volume fraction has not been fully studied. Many experimental have been conducted at low particle volume fraction (i.e. $\phi < 1\%$). As for the Reynolds number (Re), it is revealed that lateral migration of particles markedly occurs even at very low Re[4]. However, the distribution of the particle in the same micro channel will be different with the change of Re[5].

Focusing phenomenon could improve the method of separation process using microfiltration. Microfiltration is widely used for the separation process which removes contaminants from a fluid by passage through a micro porous membrane. Unfortunately, the performance of this process is always limited by the formation of a cake at the filter surface. As the particles accumulate at the surface of the filter, they will be deposited in such a way causing resistance that affect the performance of the filter. Thus, the performance of the filter will depend strongly on how particles deposited to form a cake. Beaufort et al, 2010[6] have performed filtration process at the local scale microfiltration using mixed microbial suspensions with different morphologies and sizes. The results suggested that the organization of particles was correlated to their size and shape. Since the separation of

[1]Achmad Rohyani, Philippe Schmitz, and Christine Lafforgue are with Université de Toulouse; INSA, UPS, INP; LISBP, 135 Avenue de Rangueil, F-31077 Toulouse, France, INRA, UMR792 Ingénierie des Systèmes Biologiques et des Procédés, F-31400 Toulouse, France, CNRS, UMR5504, F-31400 Toulouse, France. E-mail: achmad.rohyani@ensiacet.fr

particle suspension deals with the heterogeneity of the particle itself, controlling particle distribution before they reach the membrane surface could be an original way to understand this phenomenon. Thus, it could be enhanced by utilizing the microfluidic device.

The aim of the study is to understand the particle distribution and the degree of equilibrium position in a micro channel based on the parameters mentioned above. Experimentally, the focused particle then will be harvested using a microfiltration put perpendicularly at the end of the micro channel. By this original method, the organization of cake observed by microscope will give the information of particles position in the channel.

Combining to the experimental approach, the present work aims to study fluid flow that takes place in the original experimental device proposed to focus particles in micro channels. Numerical simulations were performed using COMSOL Multiphysics for micro channels of circular and square cross sections with different experimental conditions.

II. METHOD

A. Materials

1) Particle Suspension

Two kinds of polystyrene fluorescent microspheres with size of each particle is 4.8 μm and 1 μm and diameter density 1060 kg/m3, have been selected to model microbial particles (Thermo Scientific, USA). They were packaged at a concentration of 1% (w/w) in deionized water with trace amounts of surfactant and preservative to prevent aggregation and promote stability. Green particles (4.8 μm) emitted fluoresce at 508 nm (excitation wavelength at 468 nm) and red particles (1 μm) emitted fluorescence at 612 nm (excitation wavelength at 542 nm). These particles were diluted in filtrated water in order to get a suspension with concentration in range of 8000 and 16,000 particles /ml.

2) Membrane

In this experiment, different membrane materials were used in order to figure out the influence of the property of the membrane in filtration process. The types of the membrane utilized are shown in table 1.

B. Experimental Set-up and Method

1) Set Up

A specific experimental device was designed for this study (Fig. 1). It consisted in two branches. In the first one was flowing the diluted suspension-that was filled in a 8ml stainless steel syringe (8.5mm diameter) (HARVARD Apparatus®). The syringe was pushed by a syringe pump HARVARD® 1000 through a plastic tube of inner diameter equal to 0.78 mm (Swagelok®). This tube was connected to a circular micro-channel in siliconnitride POLYMICRO TEC® (inner diameter D = 75 μm). The micro channel was nested by a stainless steel tube to protect it. Two channel lengths of 5 and 60 cm were used.

The suspension flow rates were fixed according to the required Reynolds number in the channel: Re = ρ V D/μ, where ρ is the fluid density (kg.m-3). V is the fluid density in the micro-channel (m.s-1), D the micro-channel diameter (m), μ the fluid density (Pas).

In the second branch filtrated milli-Q water (0.22μm) was flowing to the filtration system. A pump with flow range between 6 to 600 rpm drive and tubing ID 0.8 mm (Masterflex, Bioblock scientific, USA) and a manometer (Mano-Thermo) were used to monitor the filtration conditions (trans membrane pressure).

The distance between the membrane and the channel outlet was controlled thanks to a micrometric screw.

2) Experimental Method

The selected microfiltration membrane was mounted in the membrane holder. The whole system was then filled with water in order to surround with water the micro channel and the created jet at its outlet to avoid local perturbations due to gas/liquid interface. The stainless steel syringe was filled with the particle suspension and mounted in the syringe pump. The micro channel position (distance to the membrane) was controlled thanks to the micrometric screw. The filtration pump was run on and its flow rate was set according to the required filtration velocity. Pressure was controlled in order to check membrane integrity. The syringe pump was then run on at the selected flow rate, during the required them to get a sufficient number of particles on the membrane. After this filtration time the membrane was removed and observed under the microscope.

The fluorescent particles deposited on the membrane surface were observed by microscope epi-fluorescent LEICA FW4000 equipped with specific filters corresponding to the excitation and emission wavelength of the particles. The magnification of the selected objective was x10.

III. RESULT AND DISCUSSION

In this section, we will display and discuss the results from the experiment, analytical and numerical solution. The purpose of this chapter is to comprehend the process involving fluid mechanics and determine the important parameters influencing the working of the system.

A. Particle Trajectory

During the filtration process, particles are transported by the fluid towards the membrane. The movement of the particle in stream depends on several mechanisms such as convection, Brownian diffusion, gravity and inertia. The effect of the gravity can be neglected as their density is very close to the density of water. The relative magnitude of Brownian diffusion and inertia compared to convection could be estimated using the two following dimensionless numbers: Peclet number, Pe and Stokes number, St.

A Peclet number is a dimensionless number that can relate the effectiveness of mass transport by advection to the effectiveness of mass transport by either dispersion or diffusion. Usually, diffusion is considered as the dominant transport mechanism for Peclet numbers smaller than 1[7].

$$\text{Pe} = \frac{advective\ transport\ rate}{diffusive\ transport\ rate} = 6\,\pi\,\mu\,U_f\,d_p^2/\,kT \qquad (1)$$

The Stokes number is defined as the ratio of the characteristic response time of a particle (or droplet) to a characteristic response time of the flow or of an obstacle. It expresses the relative importance of particle inertia to viscous drag for the evolution of the particle trajectory and can be interpreted as the ratio of the particle's response time[8]. If the Stokes number is small, that is much less than 1, it means that the particle motion is

tightly coupled to the fluid motion- that is the particle dispersal is the same as the fluid dispersal. If the Stokes number is large, the particles are not influences by the fluid- their response time is longer than the time the fluid has to act on it (the fluid time scale may be the rotation time of a characteristic eddy) and so the particle will pass through the flow without much deflection in its initial trajectory.

$$St = \rho_p \ U_f \ d_p^2 / \ 18 \ \mu_l \tag{2}$$

Where U_f is the characteristic filtration velocity, k is the Boltzmann constant and T is the temperature. Using the typical data for the considered application gives Pe > 10^3 and St < 10^{-5} and indicated that Brownian diffusion has a negligible effect on the particles motion and the particle motion is tightly coupled to the fluid motion. Therefore, on the basis of above estimates, it is assumed that particles follow the streamlines from the outlet of the capillary tube until they make contact with the membrane. Moreover, it is also assumed that the molecular interaction forces allow particles to adhere as soon as they make contact.

As the particles follow the streamlines, the degree of focused particles in the micro channel could be predicted by analyzing the magnitude of the streamline on membrane that comes from micro channel. This magnitude of streamline (projection radius) could be obtained by analytical solution and numerical solution discussed in appendix.

Figure 3 shows experimentally how particles deposited on the membrane observed with microscope epi-fluoresce. As in figure 3b represent particle deposited on the membrane when micro focalization happened in the micro channel and figure 3a when there is no micro focalization in the micro channel.

B. Parameters Influencing System

1) Diameter of the channel

In the experiment, we used two different size of micro channel. This treatment was done to see whether there is influence of the geometry of the channel in the projection radius of the particle. Characteristics of the channels are summarized in the table.

The numerical simulation was done utilizing COMSOL 4.3 in 2D asymmetric environment. The information in how we simulated that systems could be found in the appendix section. From the figure 4, we could see that we have the different profiles of the streamlines represented particle. Although it has different form of the streamlines, the result of the annular projection radius indicated that it has the same projection radius. For these two cases, the outer streamlines has a radius of 0.31 mm approximately. This phenomenon could be explained by the equation derived in appendix:

$$R_\alpha = \alpha \sqrt{\frac{2q\left(1-\frac{\alpha^2}{2}\right)}{\pi L_p \Delta P}} \tag{3}$$

From this equation, the parameter influenced the system was q which is mass rate of the channel, Lp which is the hydraulic permeability of the membrane and ΔP which is trans membrane pressure. This equation shows us that there is no influence of geometry in determining the projection radius. This implied that important parameter influenced the system was the

different energy between the external fluid, represented by trans membrane pressure, and the internal fluid, represented by mass rate and the property of the membrane. In next subsection, we could see further another parameter to prove whether this hypothesis is right or wrong.

2) Distance between channel and membrane

This parameter is tested by the simulation with objective to see the response of the streamlines from the micro channel with change of the distance.

As they have the same operating condition, the permeation velocity through the membrane will be similar. However, the response of the fluid will be different as shorter distance between micro channel and membrane; it will have shorter time for the fluid passing through this gap and then the membrane. This explained by the figure 5 that the fluid has slightly different projection. But, as their energetic level is the same, this deduced by the same applied conditions, they will have the same projection radius. The results of projection radius are presented in figure 6.

The results indicated in figure 6 strengthen the previous hypothesis implied that how the system assembled is independent in determine the size of projection radius.

3) Comparison between mass rate of the internal fluid and trans membrane pressure

This subsection has the objective to prove two parameters important involved in determining the projection radius as mentioned equation (9).

There is much information that we could extract from figure 7. In the first place, there is no geometry's effect in determine the projection radius since the projection radius of stainless steel tube is same with micro channel. This phenomenon already concluded in previous subsection. Other case, as the trans membrane pressure increase, it will decrease the projection radius of the particle. It is evident since the augmentation of trans membrane pressure imply increasing the energy in external fluid. Consequently, the raise of the energy in external fluid will overcome the internal fluid's energy. Thus, it will diminish the projection radius. In that figure, we could also see that numerical simulation has good agreement with analytical solution.

4) Comparison between mass rate of external and internal fluid

As indicated in previous subsection, the important parameter influenced the system is the different energy between the external fluid, represented by trans membrane pressure, and the internal fluid, represented by mass rate. In this subsection, we will deliver how these two parameters affect system in more fashioned way. We replace trans membrane pressure with mass rate external fluid. Hence, it will have more visible understanding in how these two forces influence the system, particularly in resulted projection radius. We use numerical in 2D axisymmetric and analytical solution to determine this variable and compare them. In analytical solution, we utilized equation (11) derived in appendix part as shown below

$$R = \sqrt{\frac{qd^2}{(4Q)}} \tag{4}$$

In which q is internal mass rate of fluid and Q is external mass rate of fluid. Assuming that the particle focalized in the wall, this implied that $\alpha = 1$.

In figure 8a, we vary the mass rate of internal fluid from 10 – 50 µl/min with the same mass rate of external fluid (Q = 8.1557 ml/min). The choice of this Q value because this value is minimum value that we can utilize in experiment for external fluid. From this figure, we could see that the projection radius increase as q increase.

A different phenomenon, but in the same sense, happens when we increase mass rate of external fluid. In figure 8b, we vary the mass rate of external fluid for the same mass rate of internal fluid (q = 10 ml/min), the projection radius decreased as mass rate of external fluid was increased. From these two figures, we conclude that the ratio between mass rate of external mass fluid and internal mass fluid has a strong effect on the size of projection radius. This analyzes also shows that the numerical solution is in good agreement with analytical solution.

5) Effect of the characteristics of membrane

The last influencing parameter involved in this system is the effect of different membrane used. In this subsection, we will study two different membranes to explain their effect on the system behavior. The characteristics of these two membranes are indicated in table 3.

As mentioned in table 3, we could see that cellulose acetate is more permeable than polyamide since the permeability constant of cellulose acetate is higher than polyamide one. As the membrane is more permeable, water will pass through membrane easily. So, with the same operating condition, the more permeable membrane will need less time to filter the same volume of fluid than less permeable membrane. This fact explains figure 9, why for polyamide membrane projection radius is higher than cellulose acetate. The discharge fluid from the system that utilized polyamide requires longer time to cross the distance between membrane and micro channel since it is less permeable. The longer the time, it will have much chance to develop the streamlines. Hence, it will have larger projection radius.

IV. Conclusion

The aim of this work was to optimize an original experimental set-up to study particle focusing in circular and square micro channel. The principle of this set-up was the projection of the particles on a microfiltration membrane put perpendicularly at the outlet of the channel. We have studied the effect of several operating parameters: mainly channel position, membrane permeability, flow rate in the system and shape and size of the particle's projection area.

From the results and discussions, we could make the following conclusions:

1. Parameters that influence the projection radius are external fluid flow, internal fluid flow, different type of the membrane and geometry of the micro channel.
2. For the same membrane, if we increase the driving force of the external fluid, it will result in reduction of the projection radius and vice versa.
3. The analytical calculation was in good agreement with the numerical calculation.
4. The micro channel should be accurately installed in the center of the system. Hence, it will produce a good projection radius without deviation.
5. The effect of geometry becomes important when we work in condition where inertia effect not significant.

All these results could help to improve the experimental setup and they also allow us to interprets future experiments of micro focusing in terms of radial position of particles in micro channels from the measurement of their projection radius.

References

[1]. Dino Di Carlo, Daniel Irimia, Ronald G. Tompkins et al,"Continuous inertial focusing, ordering, and separation of particles in microchannels," PNAS, vol. 104, no. 48. Site: www.pnas.org/cgi/doi/10.1073/pnas.0704958104. 2007.

[2]. Young Won Kim and Jung Yul Yoo,"Transport of solid particles in microfluidic channels," Optics and Lasers in Engineering, p. 87-98. DOI: 10.1016/j.optlaseng.2011.06.027. 2012.

[3]. J.P. Matas, J.F. Morris, and E. Guazzelli," Lateral forces on a sphere," Oil and Gas Science and Technology, vol. 59, no.1, pp. 59-70. 2004.

[4]. Young Won Kim and Jung Yul Yoo," The lateral migration of neutrally-buoyant spheres transported through square microchannels," Journal of Micromechanics and Microengineering, 18, 065015, 13 p. DOI: 10.1088/0960-1317/18/6/065015. 2008.

[5]. Yong-Seok Choi, Kyung-Won Seo and Sang-Joon Lee," Lateral and cross-lateral focusing of spherical particles in a square microchannel," Lab Chip, 11, 460-465. DOI: 10.1039/c01c00212g. 2011.

[6]. Sandra Beaufort, Sandrine Alfenore and Christine Lafforgue," Use of microfluorescence microorganisms to perform in vivo and in situ local characterization of microbial deposits," Journal of Membrane Science, 368, 30-39. DOI: 10.1016/j.memsci.2010.11.023. 2011.

[7]. Marijne Huysmans and Alain Dassargues," Review of the use of Peclet numbers to determine the relative importance of advection and diffusion in low permeability environments," Springer-Verlag. 10.1007/s10040-004-0387-4. 2004.

[8]. N. Raju and E. Meiburg," The accumulation and dispersion of heavy particles in forced two-dimensional mixing layers. Part 2: The effect of gravity," Physics of Fluids. 1070-6631/95/7(6)/1241/24/$6.00. 1995.

[9]. J. Günther, P. Schmitz, C. Albasi and C. Lafforgue.,"A numerical approach to study the impact of packing density on fluid flow distribution in hollow fiber module," J. Membr. Sci. 348, 277-286. 2010.

[10]. Zhihao Zhang," Inertial migration for spherical particles in micro-flow channels: application to membrane filtration," Report of an internship: Biochemical engineering: INSA Toulouse: 4 July 2012.

[11]. P. Schmitz and M. Prat.,"3-D Laminar stationary flow over a porous surface with suction: Description at pore level," AIChE J. 41, 2212-2226. 1995.

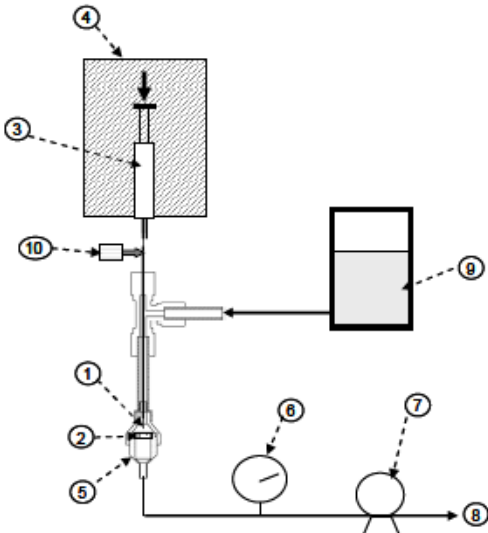Figure 1. Experimental setup,1. Circular micro-channel in a stainless steal tube; 2. Membrane; 3. 8ml syringe; 4. Syringe pump; 5.membrane holder; 6. Manometer; 7. pump; 8. Liquid outlet; 9. Water; 10. Micrometric screw
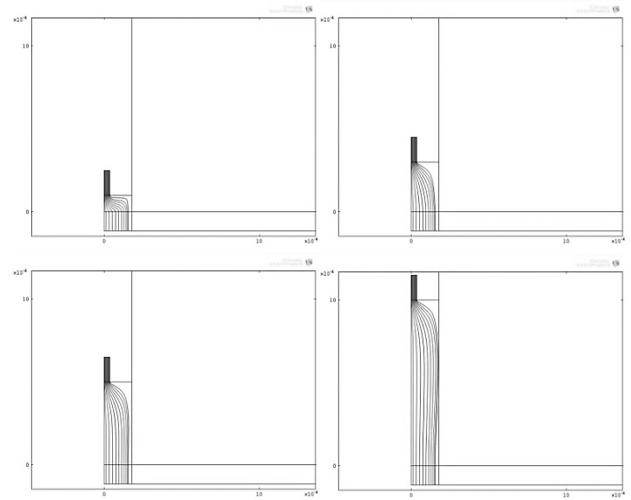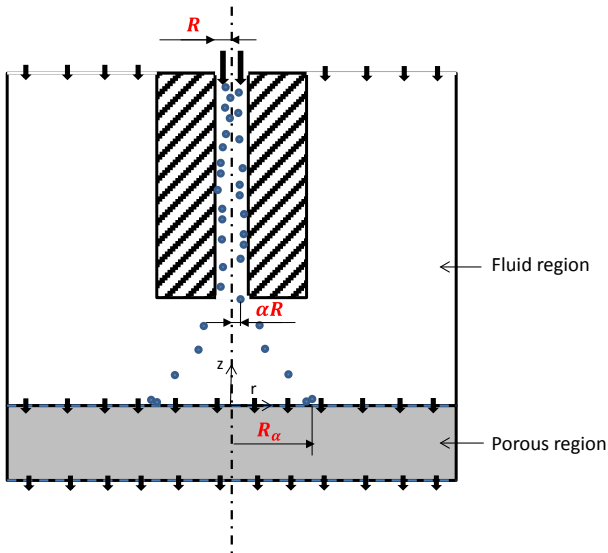

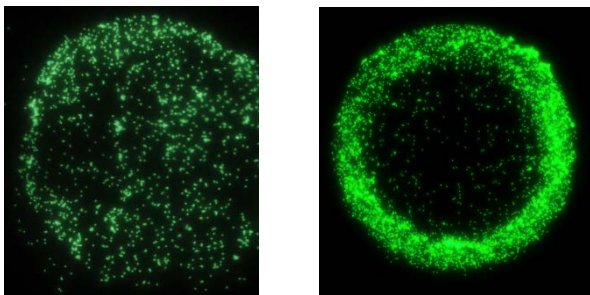Figure 2. Projection radius in circular micro channel (side view)

Figure 3. Deposition of particles on the membrane observed by microscope; a) non focused particle (left) b) focused particle (right)
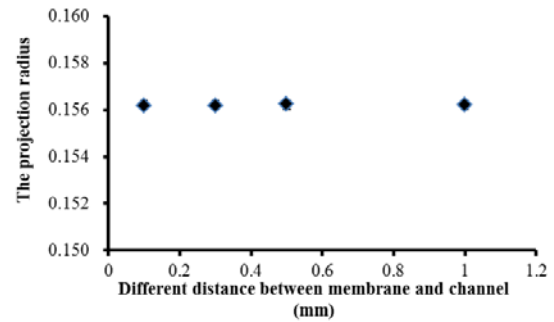

Figure 4. The projection radius in a) micro channel b) stainless tube

Figure 5. Effect of the distances between micro channel and membrane a)0.1 mm b)0.3 mm c)0.5mm d)1mm

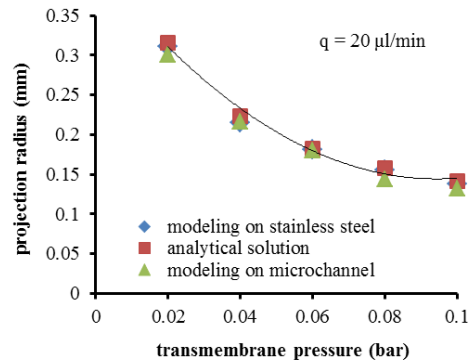Figure 6. Projection radius obtained in different distance between membrane and channel (Ho)

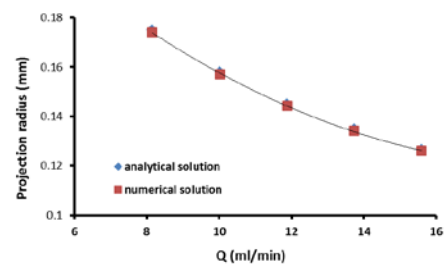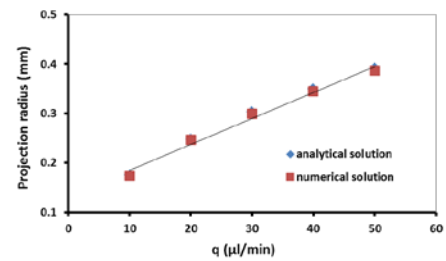
Figure 7. Projection radius versus trans membrane pressure

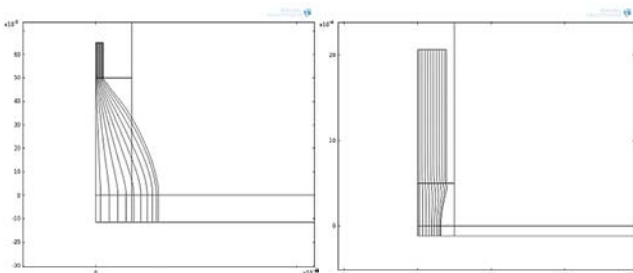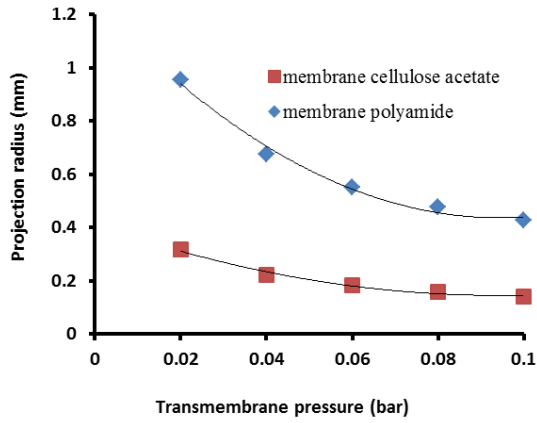Figure 8. Comparison between mass rate a) internal fluid b) external fluid

Figure 9. Projection radius versus trans membrane pressure obtained for a) Cellulose acetate b) polyamide membranes

TABLE 1.
PROPERTIES OF DIFFERENT MEMBRANE

Membrane	Pore size	Flow rate for water	Thickness
	(µm)	(ml/min/cm²/bar)	(µm)
Cellulose acetate	1.2	320	140
Polyamide	0.2	15	115
Polyamide	0.45	35	115

TABLE 2.
TWO TYPE OF CHANNELS UTILIZED IN THESE EXPERIMENTS

Type of the channel	Internal diameter	External diameter
	(mm)	(mm)
Micro channel	0.075	0.36
Stainless steel tube	0.78	1

TABLE 3.
THE PROPERTY OF THE MEMBRANE UTILIZED

Membrane	Pore size	Flow rate for water	Thickness
	(µm)	(ml/min/cm²/bar)	(µm)
Cellulose acetate	1.2	320	140
Polyamide	0.45	35	115

APPENDIX

A. Analytic calculation in determining size of particle's projection in circular micro channel

Analytical solution regarding the radius of the circular disk on the membrane could be obtained from deriving the well-known equation of Poiseuille flow. Firstly, let us consider the velocity profile of fully developed laminar flow in a micro channel with radius Ri.

$$u_z(r) = 2\frac{q}{\pi Ri^2}\left(1 - \left(\frac{r}{Ri}\right)^2\right) \quad (5)$$

where q is the flow rate of the micro channel imposed by syringe pump. Then, qα is introduced to the system as the flow rate of the micro channel with radius αR in which $0<\alpha<1$. Hence the equation (5) could be expressed as:

$$q_\alpha = \int_0^{\alpha R} u_z(r)2\pi r dr \quad (6)$$

After the integration, we could obtain:

$$q_\alpha = 2q\alpha^2\left(1 - \frac{\alpha^2}{2}\right) \quad (7)$$

Assuming that the filtration velocity at the membrane surface is uniform, hence, from the Darcy's equation, we could have

$$\frac{q_\alpha}{\pi R_\alpha^2} = L_p\Delta P \quad (8)$$

in which Lp is the hydraulic conductivity of the membrane and ΔP is the trans membrane pressure which is equal to P0 in the present problem.
Finally, rearranging the equation (7) and substituting q_α to the equation (8), we could obtain

$$R_\alpha = \alpha\sqrt{\frac{2q\left(1 - \frac{\alpha^2}{2}\right)}{\pi L_p\Delta P}} \quad (9)$$
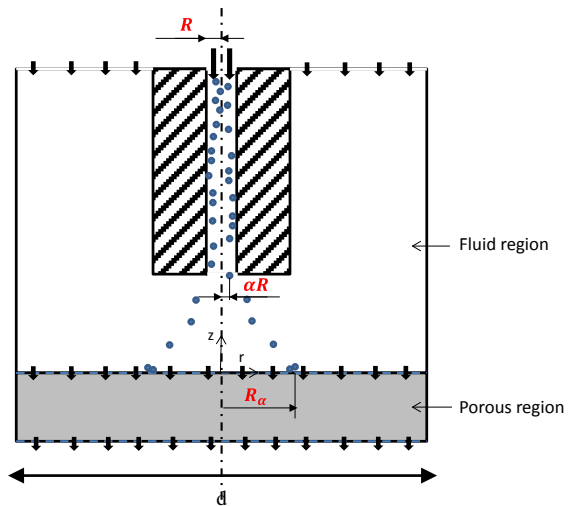

Figure 10. Projection radius in circular micro channel (side view)

We could arrange the equation 9 in order to determine the influence of external volumetric rate (Q) in respect with internal volumetric rate (q). From the Darcy's law, we have

$$\frac{Q}{\frac{1}{4}\pi d^2} = L_p\Delta P \quad (10)$$

where d is the diameter of the external tube. Assuming, that $\alpha = 1$, and substituting equation (10) to the equation (9), we could have

$$R_\alpha = \sqrt{\frac{q}{\left(\pi\frac{Q}{\frac{1}{4}\pi d^2}\right)}}$$

$$= \sqrt{\frac{q}{\left(\frac{4Q}{d^2}\right)}}$$

$$= \sqrt{\frac{qd^2}{(4Q)}} \quad (11)$$

B. Theory behind numerical calculation in determining size of particle's projection

A model based on the finite element methods was developed in a previous paper by Gunther et al (2010)[9] and Zhang (2012)[10] in 2-D to simulate numerically the flow in a dead-end hollow fiber module. An analog model is used to simulate the flow in the filtration chamber. For the sake of clarity we briefly recall the governing equations and the associated boundary conditions of the aforementioned model.
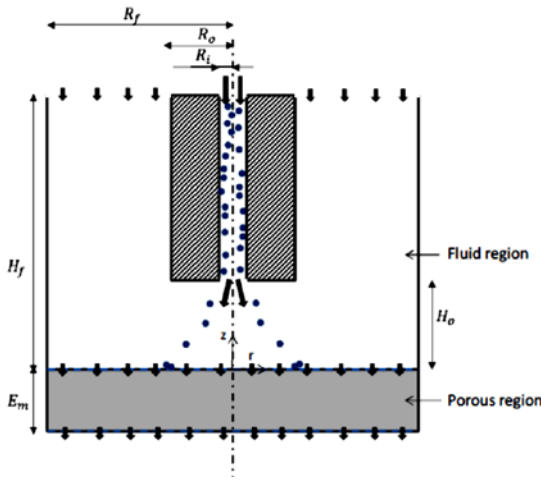

Figure 11. Scheme of the computational domain (scales not respected)

To simplify the numerical simulation, we consider an axisymmetric domain that is justified by the geometry of the filtration chamber. Therefore the flow and the subsequent particle transport and deposition can be assumed to be axisymmetric. Thus the domain consists of: (i) a cylindrical fluid region (the chamber) of height H_f and radius R_f in contact with (ii) a cylindrical porous region (the membrane) of same radius R_f, height E_m and permeability K_m (according to the given hydraulic conductivity of the membrane) and (iii) a small capillary tube of inner radius R_i and the outer radius R_0 as depicted in figure 11. The distance between the exit of the capillary tube and the membrane is H_0.

We consider a stationary, laminar and incompressible flow of a Newtonian fluid in the fluid region "f". The Navier-Stokes equations govern the mass and momentum balances:

$$\nabla . u^f = 0 \tag{12}$$

$$\rho(u^f . \nabla u^f) = -\nabla p^f + \mu \nabla^2 u^f \tag{13}$$

where ρ is the fluid density, μ is the fluid dynamic viscosity, p is the pressure, and u is the velocity vector. The flow in the porous domain "p" is ruled by the Darcy Brinkman equation as follows:

$$\frac{\rho}{\varepsilon} \frac{\partial u^p}{\partial t} + \mu_{eff} \nabla^2 u^p - \nabla p^p - \frac{\mu}{K_t} u^p = 0 \tag{14}$$

Where μ_{eff} is the effective dynamic viscosity, commonly considered as $\frac{\mu}{\varepsilon}$, ε representing the porosity and K_t is the intrinsic permeability of the porous domain. It is noted that the Darcy model is perfectly adequate to model fluid flow in porous media. However, the Darcy Brinkman model is preferred when coupling fluid and porous flow problems, in particular in the transition region where the continuity can thus be preserved for u and its derivatives.

The associated boundary conditions were chosen with respect to experimental conditions, i.e. constant working pressure in the filtration chamber, where overall pressure difference between inlet and outlet is specified and prescribed flow rate Q at the inlet of the capillary tube. It is also assumed that there is no slip condition at the fluid/ porous interface (Schmitz and Prat, 1995)[11]. Finally, the whole boundary conditions with respect to r and z axis, summarized in figure 11, can be written as:

1) Fluid region

$$p^f\left(R_0 \le r \le R_f, z = H_f\right) = P_0 \tag{15}$$

$$u_r^f\left(0 \le z \le H_f, r = R_f\right) = 0 \tag{16}$$

$$u_z^f\left(0 \le z \le H_f, r = R_f\right) = 0 \tag{17}$$

$$u_r^f\left(H_0 \le z \le H_f, r = R_0\right) = 0 \tag{18}$$

$$u_z^f\left(H_0 \le z \le H_f, r = R_0\right) = 0 \tag{19}$$

$$u_r^f\left(z = H_0, R_i \le r \le R_0\right) = 0 \tag{20}$$

$$u_z^f\left(z = H_0, R_i \le r \le R_0\right) = 0 \tag{21}$$

$$u_r^f\left(z = H_f, R_i \le r \le R_0\right) = 0 \tag{22}$$

$$u_z^f\left(z = H_f, R_i \le r \le R_0\right) = 0 \tag{23}$$

$$u_r^f\left(z = H_f, 0 \le r \le R_i\right) = 0 \tag{24}$$

$$u_z^f\left(z = H_f, 0 \le r \le R_i\right) = -\frac{2Q}{\pi R_i^2}\left[1 - \left(\frac{r}{R_i}\right)^2\right] \tag{25}$$

2) Porous region

$$p^p\left(z = -E_m, 0 \le r \le R_f\right) = 0 \tag{26}$$

$$u_r^p\left(r = R_f, -E_m \le z \le 0\right) = 0 \tag{27}$$

$$u_z^p\left(r = R_f, -E_m \le z \le 0\right) = 0 \tag{28}$$

3) Porous/ fluid interface

$$u_r^p\left(z = 0, 0 \le x \le R_f\right) = u_r^f\left(z = 0, 0 \le x \le R_f\right) \tag{29}$$

$$u_z^p\left(z = 0, 0 \le x \le R_f\right) = u_z^f\left(z = 0, 0 \le x \le R_f\right) \tag{30}$$

$$p^p\left(z = 0, 0 \le x \le R_f\right) = p^f\left(z = 0, 0 \le x \le R_f\right) \tag{31}$$

Where the subscripts r and z indicates the radial and longitudinal velocity components, respectively.